JOURNAL OF VIROLOGY, Apr. 1980, p. 178-186
0022-538X/80/04-0178/09$02.00/0

Vol. 34, No. 1

Viral DNA in Bursal Lymphomas Induced by Avian Leukosis Viruses

PAUL NEIMAN,[1,3]* L. N. PAYNE,[2] AND ROBIN A. WEISS[1]

Imperial Cancer Research Fund Laboratories, Lincoln's Inn Fields, London WC2A 3PX, England[1]; Houghton Poultry Research Station, Houghton, Huntingdon, Cambridgeshire, England[2]; and Fred Hutchinson Cancer Research Center, Seattle, Washington 98144[3]

Avian leukosis viruses (ALV) induce malignant lymphoma of the bursa of Fabricius. Viral DNA in tumors and normal tissues from infected birds were analyzed by using restriction endonucleases. Viral DNA fragments diagnostic of the exogenous ALV were easily detected in tumors, uninvolved bursal tissue, kidney, and erythrocyte nuclei. Exogenous viral DNA was more difficult to detect in liver. Using a restriction endonuclease (*Sac*I) which cleaves linear unintegrated ALV DNA in a single site to define integration sites in DNA from the various tissues, we were able to detect ALV DNA only in tumor tissue. We concluded that the proviral DNA detected in the various nontumor tissue must be integrated in multiple sites. The appearance of ALV integration sites uniquely in tumors suggests that they are clonal growths. Furthermore, the data suggested the presence of a single exogenous integration site for the ALV provirus in each of six early neoplastic bursal nodules. This provirus appeared to retain the organization of *Eco*RI and *Bam*HI recognition sequences present in the genome of virus used to infect the birds. The ALV integration site appeared different in each of the tumors studied. In a widespread metastatic lymphoma, multiple ALV integration sites were found as well as structural alterations in at least some copies of the ALV provirus.

Malignant lymphomas of the bursa of Fabricius (lymphoid leukosis) are common neoplasms in domestic chickens. The induction of these tumors is closely associated with infection by avian leukosis viruses (ALV). The genome of this class of avian retroviruses encodes the genes known to be required for viral replication, but no viral gene(s) mediating induction of bursal lymphomas or the short list of other less common neoplastic diseases (e.g., nephroblastomas and erythroleukemia) associated with these agents has been identified. The mechanisms underlying tumor induction by ALV remain obscure. The genome of ALV is closely related (about 85% homology) to that of genetically transmitted endogenous retroviruses of chickens exemplified by Rous-associated virus type 0 (RAV-0) (14). RAV-0, however, appears to lack the oncogenic potential of ALV (10). The majority of sequence divergence that does exist between ALV and RAV-0 is concentrated in the 3' end of the genomes of these agents (3, 13). The significance, if any, of this region of divergence with respect to the biological differences between these viruses remains to be established.

In the field, ALV is often spread by congenital infection of embryos by viremic hens (2). Experimentally, newly hatched susceptible chicks can be infected by intraperitoneal injection. Viral replication has been observed in many organs after infection, but the development of lymphomas is absolutely dependent upon the presence of the bursa of Fabricius (5, 15). The earliest recognizable change in the bursa is the accumulation of lymphoblasts within individual follicles (5). We have observed such transformed follicles in the majority of infected birds as early as 30 days after hatching and infection (P. E. Neiman, L. N. Payne, and R. A. Weiss, in Virus in Naturally Occurring Cancer, in press). In the study cited, we found that the vast majority of the 10 to 100 such transformed follicles per infected bursa did not appear capable of progressive growth. In fact, these structures disappeared with the physiological regression of the bursa 5 to 6 months after hatching. A much smaller number (zero to two per bursa) of discrete but progressively growing neoplastic nodules appeared beginning 14 to 15 weeks after infection. These tumors were composed of the same type of pyroninophilic lymphoblasts which appeared in transformed follicles. That the progressively growing nodules arise from the larger population of transformed follicles seems a reasonable speculation. These nodules grow rather slowly for a period of weeks. They presumably are the pre-

cursors of the rapidly growing metastatic bursal lymphomas which kill most susceptible birds between 20 and 40 weeks after hatching and infection. Thus at least three distinct stages can be observed in the development of bursal lymphomas.

In a previous study, hybridization reactions between genomic viral RNA and cellular DNA in solution were used to detect ALV-specific proviral DNA sequences in bursas and bursal tumors from infected chickens (14). On the basis of the kinetics of hybridization, there are an average of one to two copies of ALV proviral DNA per haploid genome in bursal lymphoma cells. In the present study, we have extracted DNA from early bursal nodules, from widespread bursal tumors, and from a series of other tissues from infected chickens. Viral DNA was analyzed, after digestion with a series of restriction endonucleases, by the Southern transfer technique (17). The data provide further information on the distribution of ALV DNA in infected birds, the clonal origin of bursal nodules, and the structure of the ALV provirus and adjacent host sequences in bursal lymphomas.

MATERIALS AND METHODS

Viruses and chickens. The virus used for this experiment was ALV 5938, a field isolate which has been characterized in detail in terms of both its oncogenicity and its extensive sequence homology with laboratory strains of ALV such as RAV and transformation-defective (td) deletion mutants of Rous sarcoma virus (RSV) (11, 14). We used 10^4 interference units of ALV to infect by intraperitoneal injection newly hatched chicks from a mating between susceptible (to both infection and leukosis) inbred line 15I males and outbred brown leghorn hens. Birds were sacrificed at intervals and examined for the appearance of bursal nodules, bursal lymphomas, and other neoplasms such as nephroblastomas (which were found in two instances). The course of development of neoplastic change in this experiment, as monitored by histological examination of serial sections of bursae, is described elsewhere (Neiman et al., in press). Individual neoplastic bursal nodules were dissected free of surrounding normal bursal tissue. Bursal nodules, lymphomas, and nephroblastomas and normal bursa, kidney, erythrocytes (RBC), and liver were all collected for DNA extractions.

DNA extraction. DNA was prepared from RBC nuclei on the day of collection. RBC from about 2 ml of blood were washed in TNE (0.01 M Tris-hydrochloride [pH 7.4]–0.1 M NaCl–0.001 M EDTA) and suspended in 0.01 M Tris-hydrochloride (pH 7.4)–0.01 M NaCl–0.005 M $MgCl_2$–1% Nonidet P-40. After brief blending in a Vortex mixer, nuclei were pelleted and washed two to four times in TNE until the hemoglobin was removed. The nuclei were then suspended in about 5 ml of 0.01 M Tris-hydrochloride (pH 7.4)–0.001 M EDTA (TE). Proteinase K and sodium dodecyl sulfate (SDS), were then added to 200 μg/ml and 0.5%, respectively, and the mixture was incubated at 37°C for about 2 h, or until the solution was clear. The solution was then extracted with an equal volume of chloroform-isoamyl alcohol (24:1), and the aqueous phase was obtained after centrifugation at 10,000 × *g* for 10 min. After precipitation with 2 volumes of ethanol, the DNA was spooled on a glass rod, dissolved in TE, and digested for 30 min with 20 μg of RNase A per ml (Worthington Biochemicals Corp.) at 37°C. This was followed by another 2-h digestion with proteinase K as before, extraction with an equal volume of chloroform-phenol (1:1), extraction with an equal volume of chloroform-isoamyl alcohol, and dialysis with three changes of 2 liters of TE. If necessary, DNA was concentrated to about 1 mg/ml by respooling and dissolution in TE.

DNA from sources other than RBC was usually extracted from tissues frozen and stored at −20°C. This was done by slicing the tissue while still frozen into small slivers with a scalpel and dispersing the cells in a small volume of cold saline-EDTA (0.1 M NaCl–0.1 M EDTA, pH 7.4), using a single stroke in a chilled Dounce homogenizer. This suspension was added to saline-EDTA containing 1% SDS preheated to 60°C (total volume, 5 ml/g of original tissue) and incubated for 10 min. The mixture was then cooled to room temperature, made 1 M in sodium perchlorate, and extracted with chloroform-isoamyl alcohol as for the RBC nuclear DNA preparations. The remainder of the procedure was also the same as that used for the RBC DNA.

Preparation of unintegrated ALV 5938 DNA. Twenty subconfluent plates of chicken embryo fibroblasts were infected with ALV at a multiplicity of infection of about 1. At 40 h after infection, the cells layers were rinsed with cold TNE, scraped into centrifuge tubes with a rubber policeman, and washed twice more with cold TNE. Cells were lysed with SDS and fractioned by precipitation in the cold in the presence of 1 M NaCl according to the procedure described by Hirt (6). The supernatant fraction (Hirt supernatant) containing unintegrated viral DNA was digested with RNase A and proteinase K, extracted with chloroform-phenol, and precipitated with ethanol as previously described (13). When analyzed on 0.7% agarose gels by Southern transfer and hybridization to ^{32}P-labeled viral complementary DNA (cDNA) as described later, these preparations contained predominantly a 5.1 × 10^6-dalton linear viral DNA molecule and a small amount (roughly 0.1 of the amount of linear form) of a supercoiled viral DNA molecule (data not shown). When portions representing 1 × 10^6 to 2 × 10^6 fibroblasts in the original infected cultures were used in subsequent experiments (e.g., Fig. 1A), nearly all of the detected viral DNA was contributed by the linear molecule.

Restriction endonuclease digestion and electrophoresis of viral DNA. Restriction endonucleases *Eco*RI, *Sac*I, *Bam*HI, and *Hpa*I were obtained from New England Biolabs. Digestions, carried out in 50 μl of the recommended buffer solution, contained either 10 μg of cellular DNA preparation or a portion of the Hirt supernatant DNA preparation representing about 2 × 10^6 infected fibroblasts along with 1 to 5 U of the appropriate restriction endonuclease. One mi-

crogram of lambda phage DNA was dissolved in 5-μl (0.1 volume) portions of the complete reaction mixture, and both mixtures were incubated for 2 to 4 h at 37°C. The small reaction containing the lambda DNA was analyzed by agarose gel electrophoresis (as described below) to confirm that the reaction had gone to completion. Only limit digests were analyzed further. The main reaction mixture was reduced in volume by evaporation in a vacuum, redissolved in 50 μl of 0.01 M Tris-hydrochloride (pH 7.4)–0.001 M EDTA–0.1% SDS–50% glycerol containing bromophenol blue, and loaded on a 0.4-cm-thick 1.1% horizontal agarose (Seakem) gel. Electrophoresis was at 15 V/cm for about 24 h.

Transfer to nitrocellulose membranes and hybridization. DNA was transferred to nitrocellulose membranes (0.1 μm; Sartorius) by the blotting technique described by Southern (17). Membranes were dried in a vacuum oven at 80°C for 2 h and prehybridized for 16 h at 42°C in 5× SSC (SSC = 0.15 NaCl plus 0.015 sodium citrate), 50% formamide containing Denhardt solution (0.02% albumin, Ficoll, and polyvinylpyrrolidone), 20 μg of single-stranded calf thymus DNA per ml, and 50 μg of yeast RNA per ml. The membrane was then transferred to a second plastic envelope containing the same buffer plus 10^6 cpm of a ^{32}P-labeled viral cDNA probe. The latter was prepared by in vitro reverse transcriptase reactions using purified ALV 3958 35S genomic RNA as template prepared as described previously (12) and limit DNase I-digested calf thymus DNA oligomers as primer (19). Reaction conditions and isolation of cDNA were essentially as described previously (1978). Hybridization was carried out for 48 to 72 h. The membrane was then washed in 200 ml of 2× SCC in Denhardt solution for 20 min at room temperature followed by 200 ml of 0.1× SSC–0.1% SDS at 50°C with shaking for 1 h. Final washing was with four to six rapid changes of 0.1× SSC followed by air drying. Viral DNA bands were then visualized by radioautography in the presence of calcium tungstate intensifying screens.

RESULTS

Digestion of viral and cellular DNA with *Eco*RI. Shank et al. (16) have recently reported that *Eco*RI cleaves the linear forms of both parental and td RSV unintegrated DNA very close to both the 3′ and 5′ ends of the molecule owing to the presence of a recognition site within a 300-nucleotide repeated sequence at each terminus. Two additional internal sites are recognized, giving a characteristic three-band pattern of internal fragments released by digestion of RSV and td RSV DNA with *Eco*RI. Given the extensive sequence homology between ALV 5938 and td RSV (11), it was not surprising that digestion of the linear form of unintegrated ALV DNA yielded three fragments: 2.5×10^6, 1.65×10^6, and 0.9×10^6 daltons (Fig. 1A, lane HS). These sizes are reasonably close to predicted values from the *Eco*RI map of td RSV (16). We assumed, therefore, that these three fragments represented three internal fragments of ALV, the terminal fragments being too small to detect by this method.

Figure 1 also shows the results of digestion of a series of tissues from tumor-bearing birds with *Eco*RI. In Fig. 1A, digests of DNA from two individual bursal nodules (T^a and T^b), from nontumorous portions of the bursa, and from RBC and the liver of one bird (2989) are shown. Viral DNA fragments of 2.5×10^6, 1.65×10^6, and 0.9×10^6 daltons were easily detected in all tissues except the liver, where only the largest fragment was easily observed. This fragment is commonly observed in *Eco*RI digests of DNA from uninfected chicken cells (e.g., Fig. 1, bird 2407), and it, along with the other higher-molecular-weight viral DNA-containing fragments, were considered to represent endogenous ALV-related sequences. We concluded that the liver was not extensively infected with ALV, whereas all of the other tissues contained easily detectable quantities of exogenously introduced ALV DNA. Furthermore, comparison of the tissue-derived viral DNA bands with those of linear DNA from ALV 5938 (lane HS) showed that most of proviral DNA in infected tissues, including the tumors, had the same *Eco*RI map as the original infecting virus.

Figure 1B demonstrates the results of *Eco*RI digestion of DNA from the tissues of three more birds. RBC and bursal DNA from an uninfected control bird (2407) lacked exogenous ALV *Eco*RI 1.65×10^6- and 0.9×10^6-dalton fragments, whereas DNA from RBC, bursa, and bursal nodule (T^f), but not from the liver, of infected bird 2999 contained the standard exogenous ALV *Eco*RI fragments. This figure also shows the results of digestion of DNA from RBC and an advanced widespread bursal lymphoma which appeared in chicken 2902. In this case, in addition to the standard viral *Eco*RI bands, a new viral DNA containing fragment of 2.3×10^6 daltons is clearly seen in the *Eco*RI digest of tumor DNA, but not in the RBC DNA. This observation with the metastasizing tumors was not repeated in analysis of DNA from six bursal nodules from this experiment where unusual *Eco*RI fragments did not appear. For example, an *Eco*RI digest of bursal nodules T^c and T^d and other tissues from bird 2993 yielded the standard ALV-specific internal fragments (Fig. 1C). In this case, we probed the organization of ALV DNA in the tumors and other tissues further by digestion with a second restriction endonuclease, *Bam*HI. In all tissues, two small viral DNA fragments of 1.1×10^6 and 1.5×10^6 daltons were detected which corresponded to the expected internal fragments released from ALV linear

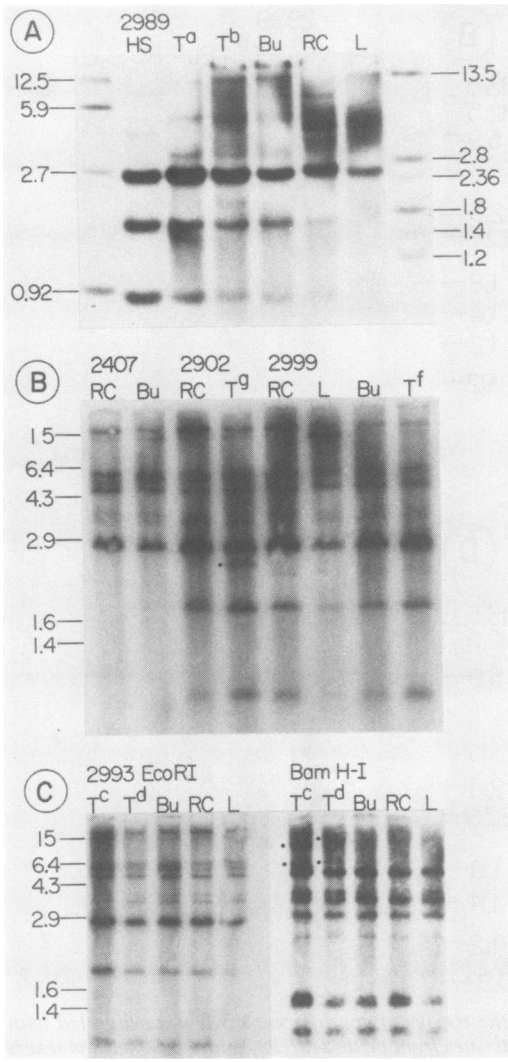

FIG. 1. *Analysis of viral DNA with EcoRI and BamHI. DNA preparations from various tissues of individual ALV-infected birds were digested with the restriction endonuclease, subjected to electrophoresis on agarose gels, and transferred to nitrocellulose membranes. Viral DNA-containing fragments were located by hybridization to ^{32}P-labeled ALV cDNA probes and radioautography. (A) Outer lanes are ^{32}P-labeled size markers (× 10^{-6} daltons) of adenovirus type 2 DNA digested with either XbaI (left) or EcoRI (right). HS is an EcoRI digest of ALV linear unintegrated DNA from a Hirt supernatant fraction of infected fibroblasts. In bird 2989, DNA was analyzed from two distinct neoplastic tumor nodules (T^a and T^b), normal uninvolved bursa (Bu), RBC nuclei (RC), and liver (L). (B) Size markers used were HindIII fragments of phage DNA (not shown). Bird 2407 was an uninfected control. Bird 2902 was infected and had a metastasizing malignant lymphoma (T^g). Bird 2999 had a single bursal nodule (T^f). The remainder of the lane designations are as for (A). The dot denotes a unique tumor-specific fragment. (C) Analysis with both EcoRI and BamHI of DNA from tissues from bird 2993. There were two distinct bursal nodules in this bird, T^c and T^d. The markers and lane designations are as before. The dots denote tumor-specific fragments.*

DNA by *Bam*HI digestion (data not shown). Therefore, the three *Bam*HI sites and the four *Eco*RI sites present in the genome of the ALV used for infection appear to be preserved in the ALV DNA detected in the various infected tissues and tumors studied in this experiment.

Digestion of viral and cellular DNA with *Sac*I. We observed that *Sac*I (and its isoschizomer *Sst*I) cleaved linear ALV DNA at a single site, yielding two fragments of 4.8×10^6 and 0.25×10^6 daltons. Therefore, *Sac*I digestion of integrated proviral DNA which is coextensive with cytoplasmic linear viral molecules should yield only fragments covalently linked to host cell sequences. Figure 2 (panels B, C, and D, lane HS) shows the larger *Sac*I-generated fragment of unintegrated linear ALV fragment (the smaller one migrated beyond the bottom of the illustration and required very long exposure of the radioautogram in order to visualize). The position of this band can be compared with viral DNA-containing fragments observed in *Sac*I digests of DNA from the same tissues depicted in Fig. 1 except 2989 RC (Fig. 2B), where the DNA was not digested by *Sac*I. In contrast to the results obtained with *Eco*RI digests, no bands were observed in either bursa or RBC DNA which migrated at the same position as that of the *Sac*I fragment of unintegrated ALV DNA. In fact, only endogenous viral DNA fragments were detected in normal tissues. We interpreted this observation to indicate that the viral DNA molecules detected in *Eco*RI digests of DNA from bursa, RBC, and kidney (not shown) are probably integrated, but in such a large number of sites that they cannot be visualized. In bursal nodules T^a, T^b (Fig. 2B), T^c, T^d (Fig. 2C), and T^f (Fig. 2A, bird 2999), *Sac*I-generated fragments containing viral DNA were detected which were absent in the digests of both linear unintegrated DNA and DNA from infected but untransformed tissues. A pair of such fragments was detected in four of these nodules as indicated by the data in the various figures; only one distinct tumor-specific fragment was identified in T^f. These fragments may represent both halves of a single *Sac*I-digested ALV provirus linked to flanking host cell sequences, or they may represent distinct integration sites of ALV. It also seems reasonable to assume that we were able to visualize these integration sites in tumors, as

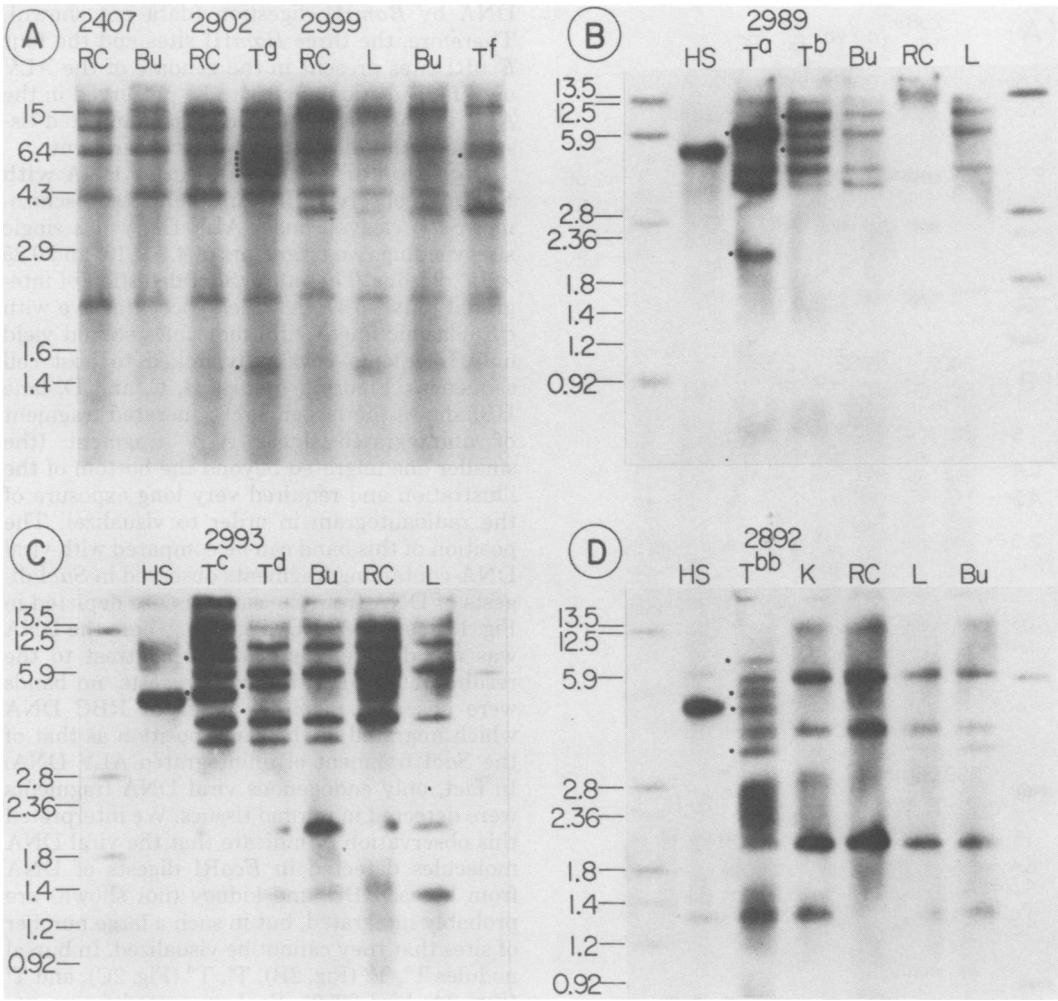

FIG. 2. *Analysis of viral DNA with SacI. DNA from the tissues of six different birds were digested with SacI and analyzed as described in Fig. 1. (A) DNA from tissues from birds 2407, 2902, and 2999 with markers and lane designations corresponding to Fig. 1B. The dots again denote tumor-specific fragments. (B) DNA from tissues of bird 2989 corresponding to EcoRI digests depicted in Fig. 1A. RBC DNA failed to digest with SacI. (C) Same analysis for DNA from bird 2993 as in Fig. 1C. (D) Analysis of DNA from tissues of a bird 2892 with a large nephroblastoma (T^{bb}). Lane K is from uninvolved kidney. The remainder of the designations correspond to our figures.*

opposed to infected but untransformed bursal tissues, because the integration site of ALV provirus is identical in each cell in the tumor. The simplest explanation for this finding is that these nodules are composed of the progeny of a single cell (that is, are clonal growths).

Figure 2A also shows *Sac*I digests of DNA from tissues of an uninfected control bird, 2407, and of DNA from RBC and tumor tissue from the bird (2902) with widspread metastatic bursal lymphoma. In the latter case, there were a large number (about six of tumor-specific ALV DNA-containing fragments. Similarly, in bird 2892, which developed a large nephroblastoma, four viral DNA-containing fragments were observed (T^{bb}, Fig. 2D) which were clearly absent in the uninvolved kidney and other tissues. The standard *Eco*RI viral DNA fragments were observed in all these tissues (not shown). Therefore other virus-induced neoplasms, such as nephroblastomas, are probably clonal growths. Furthermore, the possibility is raised that in aggressive metastatic lymphomas like T^g, there is an amplified number of integrated ALV proviruses. Since these tumors also yielded a new *Eco*RI fragment (Fig. 1B), at least one of these proviruses may

be structurally altered.

Finally, fragments of ALV containing DNA were observed of about 3.4×10^6 daltons which were variably present in *Sac*I digests of DNA from different tissues. For example, in Fig. 2, this specific fragment appears in bursal nodules and normal bursa, but not in other tissues in digests of DNA from birds 2989, 2993, and 2892 (Fig. 2B to D). In contrast, a fragment of this size was detected in all tissues of bird 2999 and no tissues from bird 2407 (Fig. 2A), as well as in other infected birds (not shown). The significance of this finding is, at present, unclear.

The data from *Sac*I digests of DNA from tissue of six different birds with bursal nodules or tumors are summarized in Table 1. All viral DNA-containing fragments observed were classified into two broad groups. Those fragments appearing in all normal and neoplastic tissues of any given bird were assigned to the category of endogenous viral information. Some of these fragments were common to all of these birds studied and presumably came from the inbred white leghorn parent. For example, bands of 13.0 $\times 10^6$, 6.0 $\times 10^6$, and 3.9 $\times 10^6$ daltons have been characterized in line 15I (1). Other fragments were variably present in different birds and were probably segregating within the brown leghorn flock. The 3.4×10^6-dalton variable fragment was assigned to this endogenous category. The remainder of the observed *Sac*I-generated viral DNA-containing fragments were tumor specific. The table lists the molecular weights of these fragments for six distinct bursal nodules, one metastasizing bursal lymphoma, and two nephroblastomas. If these fragments define the

TABLE 1. *Analysis of viral DNA with SacI*[a]

Bird no.	Endogenous[b]			Tumor specific[c]								
	All tissues		Bursa	Bursal nodules[d]						Bursal lymphoma[e]	Nephroblastoma	
				a	b	c	d	e	f	g	aa	bb
2989	13.0	8.5	Same	6.0	7.3							
	6.0		plus	2.1	4.6							
	3.9		3.4									
2993	13.0	8.5	Same			7.3	5.1					
	6.0	2.1	plus			4.8	4.0					
	3.9	1.4	3.4									
3000	13.0	8.5	Same					4.55			5.0	
	6.0	2.1						4.50			4.5	
	3.9	1.4										
2999	13.0	1.1	Same						5.5			
	6.0	8.5										
	3.9	2.1										
	3.4											
2902	13.0	8.5	NA[f]							Multiple		
	6.0	2.1								5.5–4.8		
	3.9									1.45		
2892	13.0	2.1	Same									7.0
	6.0	1.4	plus									5.4
	3.9		3.4									4.5
												3.4

[a] Data indicate the molecular weight ($\times 10^{-6}$) of *Sac*I-generated viral DNA-containing fragments. All fragments could be classed in two categories, endogenous or tumor specific. Most of the data were derived from the experiments depicted in Fig. 2.

[b] Defined as bands observed in DNA from all tissues (tumors, bursa, liver, kidney, RBC nuclei) in a particular bird.

[c] Detected only in DNA from tumor tissue.

[d] Individual small neoplastic bursal nodules dissected free of surrounding normal bursal tissue. Designations correspond to Fig. 2.

[e] Main mass of a widespread bursal lymphoma.

[f] NA, Not applicable.

integration site of ALV in the neoplastic cells, then their different sizes suggest different integration sites in each tumor. This observation appears to hold both for fragments compared on the same gel (see Fig. 2) and for distinct tumor nodules arising in the same bursa (e.g., nodules T^a and T^b in bird 2989 as well as T^c and T^d in bird 2993).

Analysis with other restriction endonucleases. One of the potential conclusions arising from the preceding analysis with *Sac*I is that the pair of tumor-specific fragments observed represented a single exogenously introduced ALV provirus in each bursal nodule examined. This conclusion might be challenged on the grounds that the small (0.25×10^6 daltons) *Sac*I fragment of linear ALV DNA might not be readily detectable even when covalently attached to adjacent host sequences, using our probe. If that were true, then all of the *Sac*I tumor-specific fragments might contain only the larger (4.8×10^6 daltons) viral segment, indicating at least two proviral copies per cell in each of the tumor nodules. Table 1 and Fig. 2 show several examples of tumor-specific fragments which are smaller than 4.8×10^6 daltons and therefore cannot be composed of a viral DNA segment of that size plus additional host cell sequences. Either these fragments must represent the smaller viral segment linked to flanking host sequences, or else some altered arrangement of ALV DNA sequences must be present. An altered arrangement was not detected in the *Eco*RI digests. To resolve this tissue, DNA from the tissues of bird 2993 was digested with two additional enzymes: *Bam*HI, which should yield both junction fragments and internals, and *Hpa*I, which cuts linear ALV DNA once near the middle of the molecule (data not shown). The results with *Bam*HI (Fig. 1C) and *Hpa*I (not shown) are summarized in Table 2. With both enzymes, a distinct pair of tumor-specific fragments was detected in each of the two bursal nodules (T^c and T^d) present in the bird. This result is also most consistent with the notion that a single provirus is present in each of the cells making up the bursal tumor nodules.

It was also of interest to determine whether DNA from the metastatic tumor (T^g) which appeared to contain several ALV proviruses when analyzed with *Sac*I contained multiple tumor-specific bands when analyzed with other enzymes. Digestion with *Hpa*I also generated multiple tumor-specific viral DNA-containing fragments (Table 2). We therefore conclude that this metastatic neoplasm is also probably a clonal growth carrying about three exogenous ALV proviruses integrated in distinct sites in the host cell genome. The simple explanation that the multiple copies are the result of the fusion of several bursal nodules in the formation of the tumor might be challenged on the groups that the *Sac*I-generated tumor-specific fragments in T^g shown in Fig. 2A (as well as those produced by *Hpa*I listed in Table 2) appear to be roughly of the same intensity as the endogenous viral bands in the same DNA. We would have expected that a mixture of cells originating from different tumor nodules would have resulted in dilution of the tumor-specific bands in compar-

TABLE 2. *Analysis with other restriction endonucleases*[a]

Endonuclease	Endogenous		Tumor specific			Exogenous internals[b]
			T^c	T^d	T^g	
2993 DNA						
*Hpa*I	13.0	5.5	3.9	3.3		
	11.0	4.2	2.8	2.5		
	8.0	2.4				
*Bam*HI	5.1	2.4	12.5	15.5		1.5
	3.9	1.4				
	3.4	1.0	6.4	6.6		1.1
	2.9					
2902 DNA						
Hpa I	13.0	4.8			14.0	
	11.0	3.6			7.5	
	6.5	2.0			5.5	
					4.0	
					3.3	
					2.4	

[a] Molecular weight ($\times 10^{-6}$) of viral DNA-containing fragments from tissues in birds 2993 and 2902 after digestion with *Hpa*I and/or *Bam*HI. Designations correspond to those in Fig. 2 and Table 1.

[b] Correspond to the fragments released from linear ALV DNA.

ison with the endogenous band present in all cells in the tumor.

DISCUSSION

These observations have led us to a number of conclusions. First, the provirus of ALV can easily be detected in the target tissues (RBC, kidney, bursa) of infected, susceptible birds. Infection of the liver appears to be less efficient than that of other tissues. Second, the provirus appears to be integrated in distinct sites in virus-induced tumors arising in these tissues. The ALV integration sites appeared different for each of nine neoplasms, six bursal nodules, one metastatic bursal lymphoma, and two nephroblastomas we examined. These findings are similar to the results of studies carried out with other retrovirus-induced neoplasms such as mammary adenocarcinomas induced by murine mammary tumor virus (4) and thymic lymphomas induced by murine leukemia virus (18). We share with these authors the conclusion that such observations suggest a clonal origin for these relatively long-latency-type tumors induced by viruses apparently lacking (at least on the basis of present knowledge) unique transforming genes.

Aided by the fact that the endogenous viral DNA-containing fragments generated by *Sac*I (or *Sst*I) from white leghorn chickens have been extensively catalogued (1), we were able to clearly separate all of the *Sac*I viral bands observed into either endogenous or tumor-specific categories (Table 1). This, in turn, allowed us to count the apparent integration sites for ALV in each tumor. There appeared to be only a single such site per locus in each of the bursal nodules. Furthermore, on the basis of the analysis with *Eco*RI and *Bam*HI, the ALV provirus occupying this site appears to have the same restriction map as the genome of bulk of the virus particles in the stock used to infect the chickens. Interestingly, the metastasizing bursal lymphoma studied in this experiment appeared to have several proviral copies integrated in different sites in the host genome. Futhermore, *Eco*RI digestion suggested a mutation in the *Eco*RI site present in proviral DNA in this tumor. Such a mutation might involve either the addition of an *Eco*RI site within the proviral DNA segment or possibly the loss of a recognition site. The possibility is thus raised that this amplification of viral DNA copies, and perhaps other changes in provirus structure, is associated with the acquisition of metastatic capability by the neoplastic bursal nodules.

We mentioned in the introduction that the mechanisms underlying induction of bursal lymphomas (or either tumor) by ALV remain obscure. The conclusions reached in this study may be examined with respect to their impact on at least some classes of mechanisms which might be involved in viral oncogenesis in this system.

For example, the idea that ALV might induce neoplastic change by integrating at a specific site in target cells is compromised by the lack of any evidence of a similarity in the integration site of ALV in the various tumors examined in this study (as well as the evidence cited in other retrovirus systems). Furthermore, the presence of a single exogenously introduced provirus for ALV in each of the bursal nodules with an apparently orthodox restriction map for *Eco*RI and *Bam*HI would seem to exclude the possibility of a large host cell sequence insert within the provirus of the kind identified with sarcoma viruses and defective acute leukemia viruses, at least at the stage of formation of bursal nodules. The situation in metastasizing lymphomas may be different. In this study, multiple ALV genomes were detected as well as alterations involving the *Eco*RI recognition site. Although the consistency of this phenomenon remains to be established, it is of interest that similar observations of viral gene amplification have been made in Moloney leukemia virus-induced thymic lymphomas in inbred BALB/Mo mice (7-9). If, indeed, metastasizing lymphomas containing several viral genomes arise from less malignant clonal tumors with single exogenous proviruses, then it seems reasonable to propose that tumor progression in this system involves one or more rounds of clonal proliferation of altered cells beyond the initial clonal expansion(s) responsible for the formation of bursal nodules. The additional proviral copies may arise simply by superinfection proceding clonal overgrowth. It is unclear at present whether this apparent viral gene amplification is a cause of tumor progression or simply a marker of clonal evolution. Continued examination of the structure of the proviral DNA in these tumors at various stages in the development of bursal lymphomas, coupled with assessment of the viral RNA and protein gene products in these cells, should continue to narrow down the list of possibilities and provide further insight into the mechanisms of oncogenesis by these agents.

ACKNOWLEDGMENTS

We thank L. Jordan and D. Macdonnell for excellent technical assistance and M. Ross for typing the manuscript.

P.E.N. is a scholar of the Leukemia Society of America and was supported by a faculty scholarship from the Josiah P. Macy Jr. Foundation. This work was also supported by Public Health Service grant CA 12895 from the National Cancer Institute.

LITERATURE CITED

1. **Astrin, S. M.** 1978. Endogenous viral genes of the white

leghorn chicken: common site of residence and sites associated with specific phenotypes of viral gene expression. Proc. Natl. Acad. Sci. U.S.A. **75**:5941–5946.

2. **Burmester, B. R., and N. F. Waters.** 1955. The role of the infected egg in the transmission of visceral lymphomatosis. Poultry Sci. **34**:1415–1429.
3. **Coffin, J. M., M. Champion, and F. Chabot.** 1978. Nucleotide sequence relationships between the genomes of an endogenous and an exogenous avian tumor virus. J. Virol. **28**:972–991.
4. **Cohen, J. C., P. R. Shank, V. L. Morris, R. Cardiff, and H. E. Varmus.** 1979. Integration of the DNA of mouse mammary tumor virus in virus infected normal and neoplastic tissue of the mouse. Cell **16**:333–341.
5. **Cooper, M. D., L. N. Payne, P. B. Dent, B. R. Burmester, and R. A. Good.** 1978. Pathogenesis of avian lymphoid leukosis. I. Histogenesis. J. Natl. Cancer Inst. **41**:373–389.
6. **Hirt, B.** 1967. Selective extraction of polyome DNA from infected mouse cultures. J. Mol. Biol. **26**:365–369.
7. **Jaenish, R.** 1976. Germ line integration and Mendelian transmission of exogenous Moloney leukemia virus. Proc. Natl. Acad. Sci. U.S.A. **73**:1260–1264.
8. **Jaenish, R.** 1979. Moloney leukemia virus gene expression and gene amplification in preleukemic and leukemic Balb/Mo mice. Virology **93**:80–90.
9. **Jahner, D., H. Stuhlman, and R. Jaenish.** 1980. Conformation of free and of integrated Moloney leukemia virus proviral DNA in preleukemic and leukemic BALB/Mo mice. Virology, in press.
10. **Motta, J. V., L. B. Crittenden, H. G. Purchase, H. A. Stone, and P. L. Witter.** 1975. Low oncogenic potential of endogenous RNA tumor virus infection or expression. J. Natl. Cancer Inst. **55**:685–689.
11. **Neiman, P. E.** 1978. Mapping by competitive hybridization of sequences which differ between endogenous and exogenous chicken leukosis viruses. Virology **85**:9–16.
12. **Neiman, P. E., S. Das, D. Macdonnell, and C. McMillin-Helsel.** 1977. Organization of shared and unshared sequences in the genomes of chicken endogenous and sarcoma viruses. Cell **11**:321–329.
13. **Neiman, P. E., C. McMillin-Helsel, and G. M. Cooper.** 1978. Specific restriction of avian sarcoma viruses by a line of transformed lymphoid cells. Virology **89**:360–371.
14. **Neiman, P. E., H. G. Purchase, and W. Okazaki.** 1975. Chicken leukosis virus genome sequences in DNA from normal chick cells and virus-induced bursal lymphomas. Cell **4**:311–319.
15. **Peterson, R. D. A., B. R. Burmester, T. M. Frederickson, H. G. Purchase, and R. A. Good.** 1964. Effect of bursectomy and thymectomy on the development of visceral lymphomatosis in the chicken. J. Natl. Cancer Inst. **32**:1343–1354.
16. **Shank, P. R., S. H. Hughes, H. J. King, J. E. Majors, N. Quintrell, R. V. Guntaka, J. M. Bishop, and H. E. Varmus.** 1978. Mapping unintegrated avian sarcoma virus DNA: termini of linear DNA bear 300 nucleotides present once or twice in two species of circular DNA. Cell **15**:1383–1395.
17. **Southern, E. M.** 1975. Detection of specific sequences among DNA fragments separated by gel electrophoresis. J. Mol. Biol. **98**:503–517.
18. **Steffen, D., and R. A. Weinberg.** 1978. The integrated genome of murine leukemia avirus. Cell **15**:1003–1012.
19. **Taylor, J. M., R. Illmenee, and J. Summer.** 1976. Efficient transcription of RNA into DNA by avian sarcoma virus polymerase. Biochim. Biophys. Acta **442**: 324–330.